**Annales
Geophysicae**

Simultaneous observation of traveling ionospheric disturbances in the Northern and Southern Hemispheres

C. E. Valladares[1]**, J. Villalobos**[2]**, M. A. Hei**[1]**, R. Sheehan**[1]**, Su. Basu**[3]**, E. MacKenzie**[1]**, P. H. Doherty**[1]**, and V. H. Rios**[4]

[1]Institute for Scientific Research, Boston College, Chestnut Hill, MA 02467, USA
[2]Department of Physics, Universidad Nacional de Colombia, Bogota, Colombia
[3]Center for Space Physics, Boston University, 725 Commonwealth Ave, Boston, MA 02215, USA
[4]Department of Physics, Universidad Nacional de Tucuman, Tucuman, Argentina

Abstract. Measurements of total electron content (TEC) using 263 GPS receivers located in the North and South America continents are presented to demonstrate the simultaneous existence of traveling ionospheric disturbances (TID) at high, mid, and low latitudes, and in both Northern and Southern Hemispheres. The TID observations pertain to the magnetically disturbed period of 29–30 October 2003 also known as the Halloween storm. The excellent quality of the TEC measurements makes it possible to calculate and remove the diurnal variability of TEC and then estimate the amplitude, wavelength, spectral characteristics of the perturbations, and the approximate velocity of the AGW. On 29 October 2003 between 17:00 and 19:00 UT, there existed a sequence of TEC perturbations (TECP), which were associated with the transit of atmospheric gravity waves (AGW) propagating from both auroral regions toward the geographic equator. A marked difference was found between the northern and southern perturbations. In the Northern Hemisphere, the preferred horizontal wavelength varies between 1500 and 1800 km; the propagation velocity is near 700 m/s and the perturbation amplitude about 1 TEC unit (TECu). South of the geographic equator the wavelength of the TECP is as large as 2700 km, the velocity is about 550 m/s, and the TECP amplitude is 3 TECu. Concurrently with our observations, the Jicamarca digisonde observed virtual height traces that exhibited typical features that are associated with TIDs. Here, it is suggested that differences in the local conductivity between northern and southern auroral ovals create a different Joule heating energy term. The quality of these observations illustrates the merits of GPS receivers to probe the ionosphere and thermosphere.

1 Introduction

During the last decade, it has become evident that a vast network of GPS receivers is a superb diagnostic of space weather due to its ability to resolve spatial-temporal ambiguities. Recently, GPS TEC measurements have detected the passage of atmospheric gravity waves (AGW) at mid and high latitudes (Ho et al., 1998a; Saito et al., 1998; Shiokawa et al., 2002), improved understanding of the dynamics of the magnetically-disturbed mid-latitude ionosphere (Basu et al., 2005), and helped the forecast of the onset of equatorial plasma irregularities (Valladares et al., 2001). The first studies of AWG using GPS receivers employed 150+ globally distributed receivers to indicate the existence of small TEC enhancements developing simultaneously at both north and south auroral regions (Ho et al. 1998a, b). These TEC enhancements moved toward lower latitudes and from the night side into the dayside. Later, Saito et al. (1998) used a denser network of over 900 receivers in Japan to reveal the spatial and temporal evolution of TIDs. The amplitude of the perturbation structures was found to be 1 TEC unit (TECU), the wavelengths up to 300 km, and with a phase velocity of order 100 m/s. Shiokawa et al. (2002) used 1000+ GPS receivers, an all-sky imager, a scanning photometer, and three sounders, all installed in Japan, to study the dynamics, propagation and source of large-scale TIDs (LSTID). Shiokawa et al. (2002, 2003) concluded that the 630.0 nm airglow intensifications, *fo*F2 and TEC perturbations were the response to an enhancement of the poleward neutral wind associated

with an equatorward propagating gravity wave. However, their data did not resolve conclusively whether the source of the gravity waves was the high latitude Joule heating or the Lorentz force associate with substorms. Joule or frictional heating of the neutral gas is produced by the difference in velocity between neutrals and ions. The Lorentz forcing consists of momentum transfer to the ions that is passed to the neutrals by collisions (ion drag) (Balthazor et al., 1997). Joule heating is a dominant mechanism at higher altitudes producing large-scale gravity waves with velocity $\sim$640 m/s that can propagate to lower latitudes whereas Lorentz forcing predominates at lower altitudes generating medium-scale gravity waves with $\sim$320 m/s velocity (Hunsucker, 1982).

It has been demonstrated that during magnetically active days large-scale waves generated in the auroral zone propagate equatorward; in contrast medium-scale GW generated by tropospheric weather systems travel mainly in the zonal direction (Hocke and Schlegel, 1996). Theoretical considerations by Hines (1967) have indicated that GWs propagate with velocities near $\sim$700 m/s and have periods that increase with travel distance from mid to low latitudes. The numerical model of Richmond (1978, 1979) suggested that the thermospheric response to a substorm consisted of disturbances propagating equatorward with a speed of about 750 m/s. Mayr et al. (1984a, b) developed a linear transfer function model to describe the different gravity wave modes and impulsive penetrations due to Joule heating. Nicolls et al. (2004) used TEC data from a network of GPS receivers in North America and vertical density profiles collected at Arecibo to examine the 3-D structure of LSTIDs. The TEC perturbations were of order 1 TEC unit and were associated with wind pulses that drove the mid-latitude F-layer up and down. On the modeling side, Balthazor and Moffett (1997) used a global fully-coupled thermosphere-ionosphere-plasmasphere model to simulate the transit of gravity waves originated from a high-latitude electric field enhancement. The thermospheric disturbance propagated toward the equator from both poles and interfered constructively at the equator producing TEC and density variations that were larger than the mid latitude perturbations.

In this paper, we present TEC perturbations observed during the major storm of October 2003 by 263 GPS receivers distributed in the North and South Americas. The TEC perturbations were generated by large-scale AGWs traveling from auroral latitudes toward the geographic equator. In the Northern Hemisphere the dense network of GPS receivers made it possible to determine the wavelength, propagation direction, and phase velocity of the LSTID. In the Southern Hemisphere, GPS receivers are installed more sparsely. Nevertheless, the south-American TEC perturbations indicate TID-related fluctuations with slightly different characteristics than their Northern Hemisphere counterpart. We also point out that the propagating waves seem to meet in a location north of the geographic equator.

2   The superstorm of October–November 2003

Between late October and early November 2003 a series of solar eruptions occurred from 3 regions of the Sun, producing a total of 80 coronal mass ejections (CMEs). During this period, the fastest CME ($\sim$2700 km/s) recorded in 30 years was observed on 4 November 2003 at 1954 UT. The solar flux of 28 October 2003 was the fourth most intense in recent history, and produced the largest TEC enhancement (25 TEC units) at the sub-solar point (Tsurutani et al., 2005). On 30 October, shortly after 18:00 UT, a tenfold enhancement in the TEC was observed over the US mainland. During this time, steep gradients were seen in the poleward boundaries of a storm-enhanced density (SED) eroded by strong sub-auroral polarization stream (SAPS) electric fields. Foster and Rideout (2005) indicated that the enhanced TEC resulted from a rapid poleward redistribution of equatorial plasma responding to the storm-time eastward electric fields. Mannucci et al. (2005) suggested that a combination of prompt penetration electric fields and diffusion along field lines driven by a super fountain effect were responsible for the peak mid-latitude density distribution.

3   Observations

Our primary data set consists of TEC values measured by 263 GPS receivers that routinely operate in North and South Americas. Equivalent vertical TEC values were calculated independently for each of the GPS receivers using an analysis code that was developed at Boston College. This computer software uses the satellite biases as reported by the University of Bern and calculates the receiver bias minimizing the TEC variability observed between 02:00 and 06:00 LT. TEC curves corresponding to each satellite pass and for each of the 263 receivers were then fitted to a 4th order polynomial to filter out the diurnal variability and to evaluate TEC perturbations (TECP) containing time scales of 3 h or less. Our method is different than the algorithm used by Shiokawa et al. (2002) that estimates the unperturbed TEC level by removing a 2-h running average, or the procedure employed by Nicolls et al. (2004) that calculates the unperturbed TEC value using a 4-h running average for several latitude-longitude bins. We claim that our derivation of the TEC perturbations reflects quite well the variability of the integrated number density due to the transit of large-scale gravity waves.

Figure 1 shows four TECP traces corresponding to two stations located in the Northern Hemisphere (Ensenada and Darlington) and two sites placed in the Southern Hemisphere (Ancon and Cuzco). The prominent feature of panels (a) and (b) is the pronounced level of coherence that starts at 17:00 UT. The latitudinal displacement of these 2 GPS stations produces a small time offset of a few minutes. We demonstrate later that the apparent motion of the TECP is
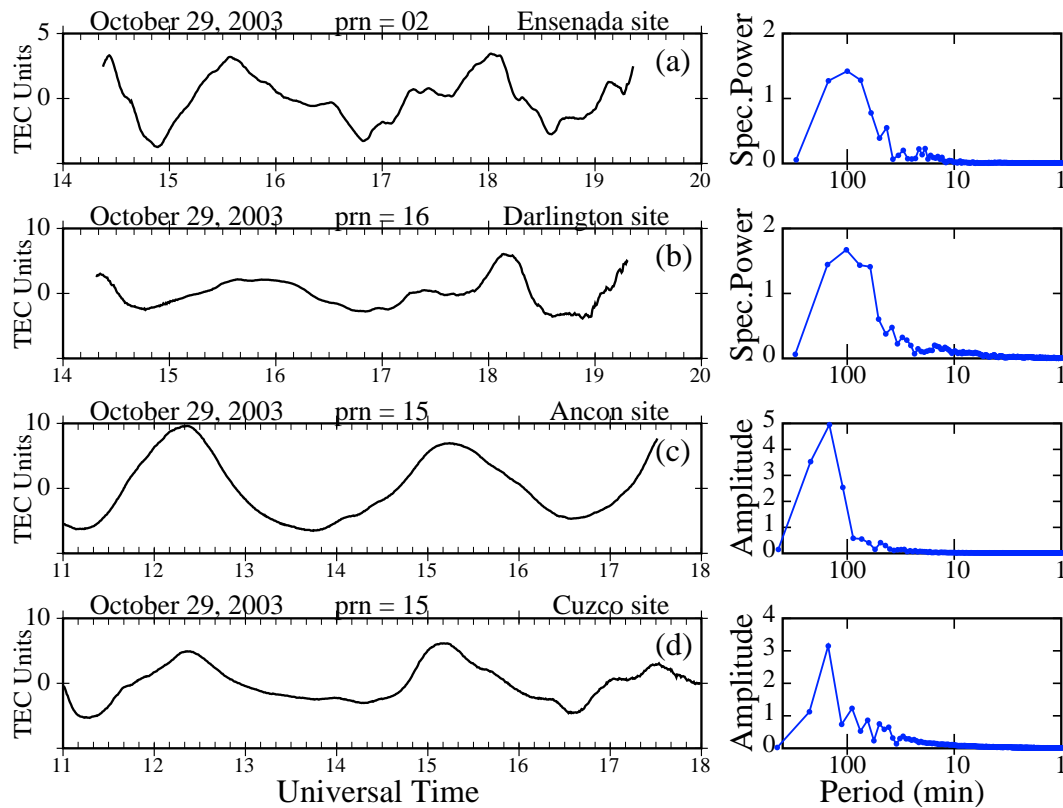
Fig. 1. The left panels show the values of the TEC perturbations observed at two stations located in the Northern Hemisphere (Ensenada and Darlington) and two stations situated in the Southern Hemisphere (Ancon and Cuzco). The right-hand panels display the power spectra of the TEC perturbations.

southward in the Northern Hemisphere with an initial phase front almost aligned with the geographic east west. The TECP traces of Fig. 1c and 1d display an almost perfect correlation, but show no offset as these stations (Ancon and Cuzco) are placed at nearly the same geographic latitude. The right side panels of Fig. 1 display the spectral power of the TECP as a function of the period. The spectra (frames a and b) of the Northern Hemisphere stations are wide and centered at 100 min. Conversely, the Southern Hemisphere TECP spectra are much narrower and centered at slightly larger time scales (150 min).

Figure 2 shows 2-min snapshots of the TEC perturbations observed on four instances separated by 10 min. They have been color coded according to the sign of the perturbation to emphasize their latitudinal extension. Each color pixel has been placed at the geographic location of the assumed 350-km altitude piercing point. Figure 2a reveals the existence of up to 5 latitudinal bands alternating between positive (blue) and negative (red) TEC perturbations. The northernmost band coincides with the US-Canada border. This is followed by negative and positive bands extending across the continental US. A fourth band is seen over Florida and Mexico only to be interrupted by lack of data over the Caribbean Sea. Further south, we observe a fifth band filling Central

America. It is important to note that in Central and South America GPS receivers are installed quite sparsely, hindering the identification of TECP bands. Figure 2b, obtained 10 min later, shows that the location of each band has shifted southward by ~4°, and a new band of positive TEC perturbations originates near the southern Canadian border. The apparent velocity of the TECP features approximates 700 m/s. Figure 2c and 2d confirms the persistence of TECP, the apparent southern motion of the TIDs, and the continuous formation of new TECP bands in the northern part of North America. Note that the TECP over Florida change colors every 15–20 min as northern TECP values apparently displace south. We also note that the phase front shows a small rotation as the perturbation "propagates" equatorward.

Figure 3 shows TECP values recorded by 10 GPS stations located near the west coast of South America. Although the apparent propagation of the TECP bands seems quite similar to the TEC perturbations observed in North America, their amplitude, wavelength, and velocity are very different. Also note that the frame-to-frame time difference in this sequence is 30 min. The symbols that are used to depict TEC perturbations are circles with radii dependent on the amplitude of the TECP. The size of the perturbations seems to grow as the perturbations are observed closer the geographic equator.
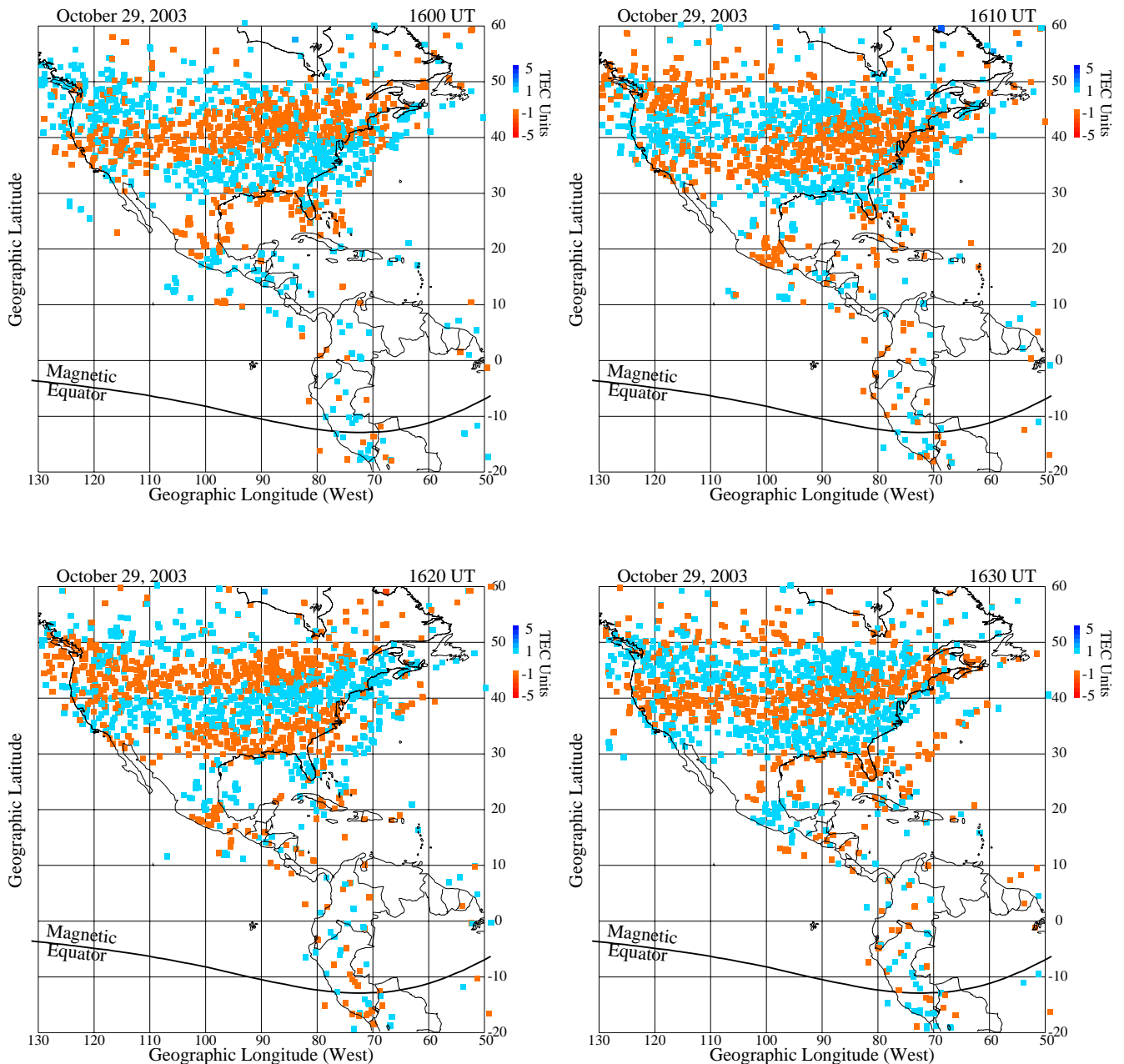
Fig. 2. Set of geographic displays of the distribution of TEC perturbations recorded in North America and the Caribbean region. Blue pixels indicate positive variations of the perturbations and red negative TECP values. Time interval between frames is 10 min. See text for details.

A 3 TECu perturbation is seen near the magnetic equator at 1854 UT, and values ∼1 TECu at a distance 20° away from the equator. In spite of the low number of points, it is evident that the Southern Hemisphere perturbations move northward with an average speed equal to 550 m/s. The latitudinal extension of the southern TECP bands is evidently larger than the Northern Hemisphere bands. They extend ∼13° in the Southern Hemisphere and only 8° in the Northern Hemisphere.

Figure 4 shows a pictorial representation of both Northern and Southern Hemisphere TEC perturbations; it serves to infer the equatorward motion of the underlying AGWs. This plot is framed in a coordinate system of geographic latitude versus universal time. This figure was obtained by integrating all the pixels measured between 60° and 90° W longitude and placing a blue or orange point depending on the sign of the result. Before 15:00 UT, a random distribution of average TECP values was obtained. Between 15:00 and 17:00 UT,
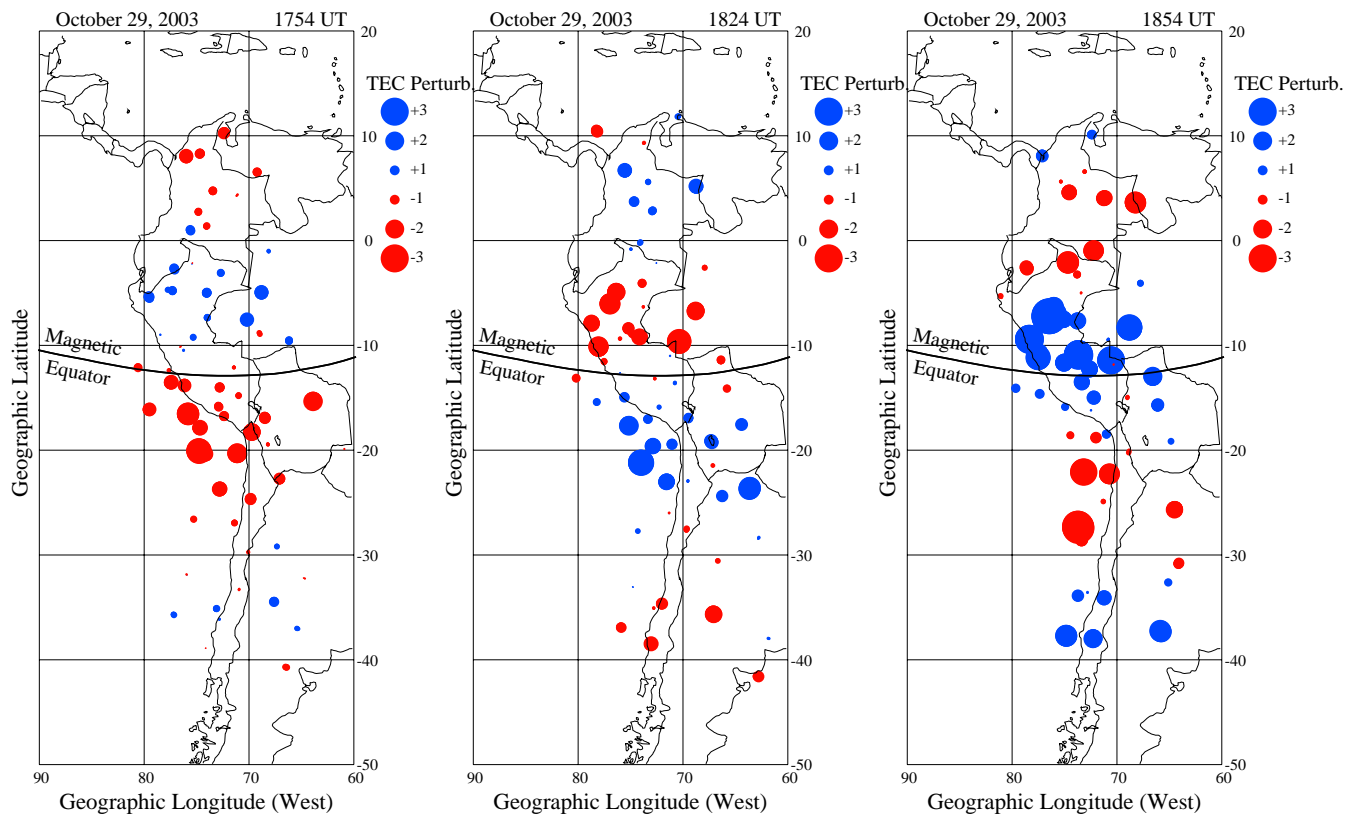
Fig. 3. Similar to Fig. 2 but for TEC perturbations observed in South America for 3 instances separated by 30 min. Note the size of the small circles indicate the amplitude of the TEC perturbations that vary between −3 and 3 TECu.

the integrated perturbations display a good degree of coherence only at high and mid latitudes. These perturbations seem to fade at ∼20° geographic latitude. After 17:00 UT, a new band seems to be propagating from the north and another from the south that meet near the geographic equator at 18:45 UT. The black lines that reach the equator at 18:45 and 19:45 UT emphasize our interpretation of the locations of the negative perturbations and the equatorward propagation of the northern and southern TECP. A second band of TEC perturbations likely originates almost simultaneously from both high latitude regions between 18:20 and 18:30 UT. They are observed to merge near the geographic equator at 19:50 UT. No propagation into the opposite hemisphere is evident during these events.

4 Discussion

During the first two days of the Halloween storm we detected TEC perturbations, similar to the ones presented here, on 2 other occasions. These two periods correspond to 06:00–09:00 UT on 29 October, and 17:00–21:00 UT on 30 October 2003. All three events developed during times of cross polar cap potential larger than 150 KV (DMSP F13 and F15). Similarly, the AE index of Fig. 5 indicates that during the

TIDs of October 2003 electrojet currents were enhanced at auroral latitudes. Shiokawa et al. (2002) have associated energy deposited in the auroral oval with the initiation of meridionally propagating gravity waves. These authors calculated the amount of high latitude Joule heating and Lorentz force. However, neither term had the necessary strength to generate a gravity wave. These authors concluded that a single wave large-scale TID was associated with the termination of the equatorward wind. The TIDs present here have characteristics that differ from the TIDs shown by Shiokawa et al. (2002). During the October 2003 Halloween storm, we observed a train of gravity waves likely generated by repetitive pulses of energy that were deposited at auroral latitudes. We believe that intense Joule heating being deposited at auroral latitudes likely produced the GWs associated with the observed TIDs. Balthazor et al. (1997) have indicated that Joule heating is associated with gravity waves containing mean velocity near 640 m/s, whereas Lorentz forcing produce waves with a lower velocity about 320 m/s. The large velocity that was observed in both hemispheres, close to 600 m/s, support the idea that intense Joule heating, as seen in the large auroral currents of Fig. 5, is likely responsible for the generation of the AGWs. Joule heating ($\boldsymbol{J} \times \boldsymbol{E}$) being proportional to the Pedersen conductivity could be different in opposite auroral
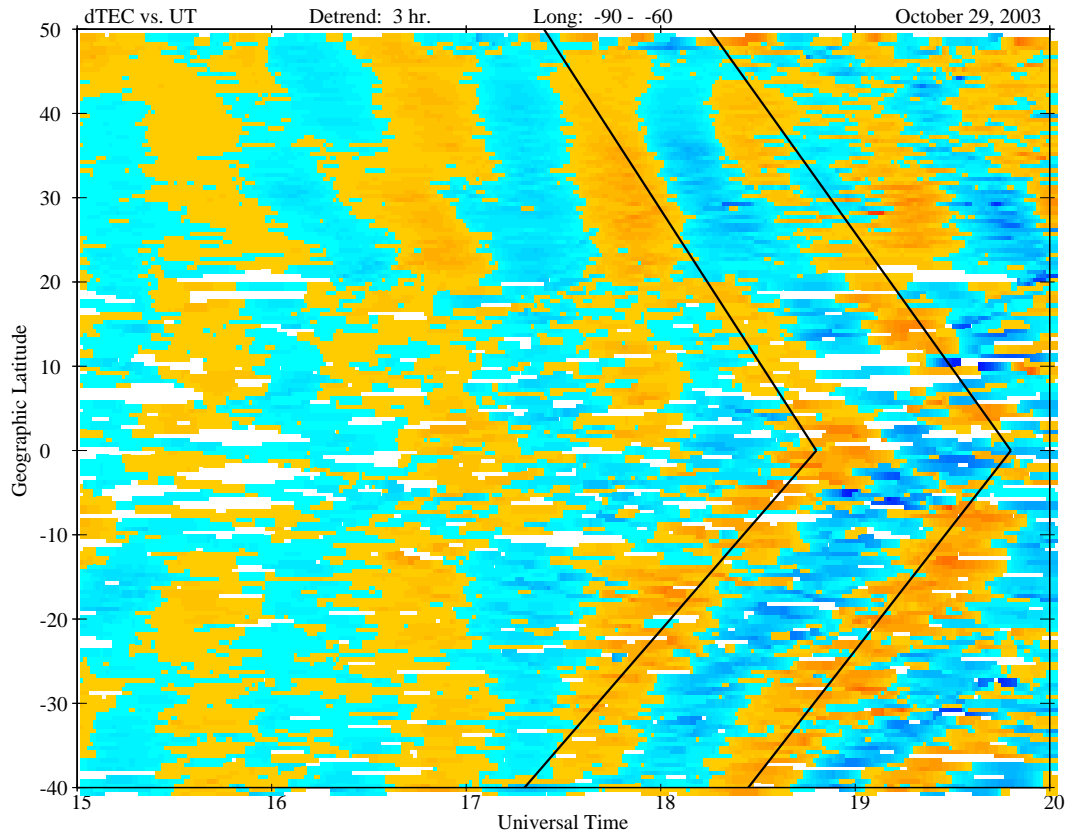
Fig. 4. Color-coded representation of the TEC perturbations in a reference frame of geographic latitude versus universal time. Each pixel indicated here corresponds to the average of the perturbations that were observed in longitude between 90° W and 60° W at the latitude and time indicated in the figure.
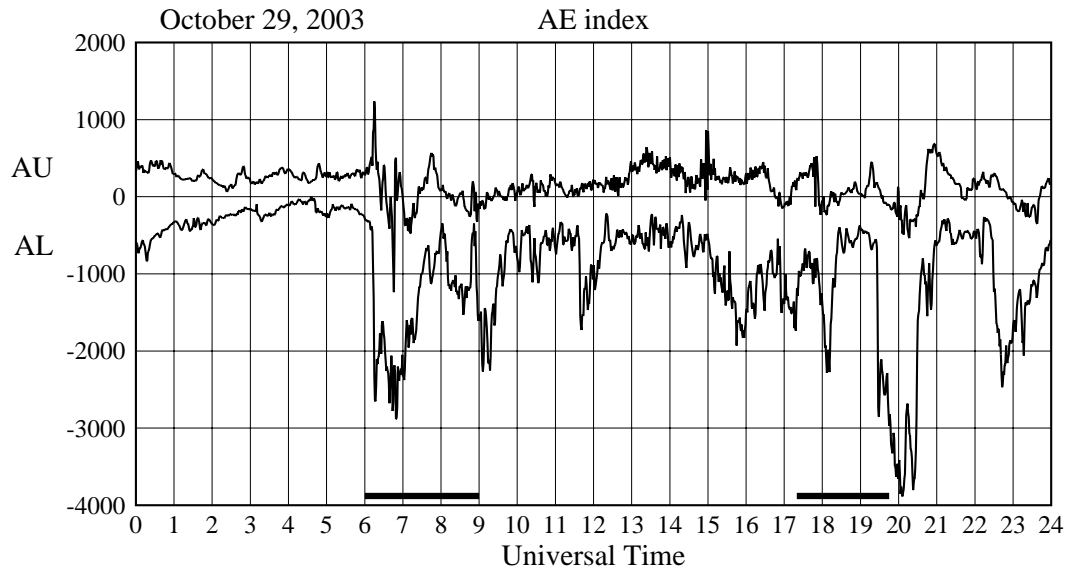

Fig. 5. This figure presents the AE index corresponding to 29 October 2003. The lines near the bottom indicate the times when TEC perturbations were detected by our analysis program.

zones due to differences in the number density. Additionally, Hajkowicz (1992) found that during magnetic storms, stronger TID signatures are created in the nighttime sector than in the sunlit region. The fact that the TEC perturbations interact at the geographic equator, instead of the magnetic equator as predicted by Balthazor and Moffett (1997), can be explained by the large difference in the gravity wave velocity in opposite hemispheres and/or the timing that the impulsive energy is released in opposite auroral zones. We are not able to resolve the time that the energy flux is deposited at high latitudes due to the limited number of observations near the auroral ovals.

We have also examined ionograms collected by the Jicamarca digisonde (not shown here) looking for signatures of TIDs. Two distinct features in the ionograms corroborate our contention that TIDs were simultaneously observed in South America. (1) The ionogram for 17:30 UT shows a clear change in the shape of the virtual height trace between 4.5 and 13 MHz. (2) The ionogram color-coded Doppler profile exhibits a shift from positive to negative as a function of frequency. The ionogram height profile indicates that the density disturbance was limited to the height range between 225 and 380 km altitude, corresponding to a half wavelength size equal to 155 km. Analysis of atmospheric wave propagation provides a dispersion relation of the form:

$$\lambda_z^2 = \left(\frac{\tau_g^2}{\tau^2 - \tau_g^2} \right) \lambda_x^2 \qquad (1)$$

where λ_x is the horizontal wavelength, λ_z is the vertical wavelength, τ is the period and τ_g is the Brunt-Väisälä period ($\sim$15 min). Using the values measured in the Southern Hemisphere, we obtained a vertical wavelength equal to 270 km. This value is in good quantitative agreement with the vertical wavelength measured by the Jicamarca digisonde.

It is necessary to mention that the perturbation spectra are mildly affected by the motion of the GPS satellites. The velocity of the sub-ionospheric penetration point of the GPS satellites is about 80 m/s. However, this effect does not change our conclusions about the time scale of the TID perturbations because the velocity of the GW is about an order of magnitude larger.

5 Conclusions

We have presented experimental evidence which indicates that the TEC perturbations are of order 1 TEC unit, that they coexist in both Northern and Southern Hemispheres, propagate equatorward, and have wavelength, phase velocities, and amplitudes that differ between hemispheres.

Our results agree with findings of theoretical simulations by Balthazor and Moffett (1997) in which the TEC perturbations interact constructively near the equatorial line. However, our observations suggest that the TEC perturbations

unite close to the geographic equator instead of the magnetic equator.

References

Balthazor, R. L. and Moffett, R. J.: A study of atmospheric gravity waves and travelling ionospheric disturbances at equatorial latitudes, Ann. Geophys., 15, 1048–1056, 1997.

Balthazor, R. L., Moffett, R. J., and Millward, G. H.: A study of the Joule and Lorentz inputs in the production of atmospheric gravity waves in the upper thermosphere, Ann. Geophys., 15, 779–785, 1997.

Basu, Su., ▮▮▮▮please name at least 3 authors!, et al.: Two components of ionospheric plasma structuring at midlatitudes observed during the large magnetic storm of October 30, 2003, Geophys. Res. Lett., 32, L12S06, doi:10.1029/2004GL021669, 2005.

Foster, J. C. and Rideout, W.: Midlatitude TEC enhancements during the October 2003 superstorm, Geophys. Res. Lett., 32, L12S04, doi:10.1029/2004GL021719, 2005.

Hajkowicz, L. A.: Universal time effect in the occurrences of large-scale ionospheric disturbances, Planet. Space Sci., 40, 1093–1099, 1992.

Hines, C. O.: On the nature of traveling ionospheric disturbances launched by low-altitude nuclear explosions, J. Geophys. Res., 72, 1877–1882, 1967.

Ho, C. M., Manucci, A. J., Sparks, L., Pi, X., Lindqwister, U. L., Wilson, B. D., Iijima, B. A., and Reyes, M. J.: Ionospheric total electron content perturbations monitored by the GPS global network during two Northern Hemisphere winter storms, J. Geophys. Res., 103, 26 409–▮▮▮▮last page number?, 1998a.

Ho, C. M., Mannucci, A. J., Lindqwister, U. J., Pi, X., Tsurutani, B. T., Sparks, L., Iijima, B. A., Wilson, B. D., Harris, I., and Reyes, M. J.: Global ionospheric TEC variations during January 10, 1997 storm, Geophys. Res. Lett., 25(14), 2589–2592, 1998b.

Hocke, K. and Schlegel, K.: A review of atmospheric gravity waves and travelling ionospheric disturbances: 1982–1995, Ann. Geophys., 14, 917–940, 1996.

Hunsucker, R. D.: Atmospheric Gravity Waves Generated in the High-Latitude Ionosphere: A Review, Rev. Geophys., 20(2), 293–315, 1982.

Mannucci, A. J., Tsurutani, B. T., Iijima, B. A., Komjathy, A., Saito, A., Gonzalez, W. D., Guarnieri, F. L., Kozyra, J. U., and Skoug, R.: Dayside global ionospheric response to the major interplanetary events of October 29–30, 2003 "Halloween Storms",

Geophys. Res. Lett., 32, L12S02, doi:10.1029/2004GL021467, 2005.

Mayr, H. G., Harris, I., Varosi, F., and Herrero, F. A.: Global excitation of wave phenomena in a dissipative multiconstituent medium, 1, Transfer function of the Earth's thermosphere, J. Geophys. Res., 89, 10 929–**last page number?**, 1984a.

Mayr, H. G., Harris, I., Varosi, F., and Herrero, F. A.: Global excitation of wave phenomena in a dissipative multiconstituent medium, 2, Impulsive perturbations in the Earth's thermosphere, J. Geophys. Res., 89, 10 961–**last page number?**, 1984b.

Nicolls, M. J., Kelley, M. C., Coster, A. J., González, S. A., and Makela, J. J.: Imaging the structure of a large-scale TID using ISR and TEC data, Geophys. Res. Lett., 31, L09812, doi:10.1029/2004GL019797, 2004.

Richmond, A. D.: Gravity wave generation, propagation, and dissipation in the thermosphere, J. Geophys. Res., 83, 4131–**last page number?**, 1978.

Richmond, A. D.: Large-amplitude gravity wave energy production and dissipation in the thermosphere, J. Geophys. Res., 84, 1880–**last page number?**, 1979.

Saito, A., Iyemori, T., and Takeda, M.: Evolutionary process of 10 kilometer scale irregularities in the nighttime midlatitude iono-sphere, J. Geophys. Res., 103(A3), 3993–4000, 1998.

Shiokawa, K., Otsuka, Y., Ogawa, T., Balan, N., Igarashi, K., Ridley, A. J., Knipp, D. J., Saito, A., and Yumoto, K.: A large-scale traveling ionospheric disturbance during the mag-netic storm of 15 September 1999, J. Geophys. Res., 107, 1088, doi:10.1029/2001JA000245, 2002.

Shiokawa, K., Ihara, C., Otsuka, Y., and Ogawa, T.: Statistical study of nighttime medium-scale traveling ionospheric disturbances using midlatitude airglow images, J. Geophys. Res., 108(A1), 1052, doi:10.1029/2002JA009491, 2003.

Tsurutani, B. T., **please name at least 3 authors!**, et al.: The October 28, 2003 extreme EUV solar flare and resultant extreme ionospheric effects: Comparison to other Halloween events and the Bastille Day event, Geophys. Res. Lett., 32, L03S09, doi:10.1029/2004GL021475, 2005.

Valladares, C. E., Basu, S., Groves, K., Hagan, M. P., Hysell, D., Mazzella, A., and Sheehan, R.: Measurements of equato-rial spread-F ionospheric conditions using a latitudinal chain of GPS receivers, J. Geophys. Res., 106, 29 133–**last page number?**, 2001.